Advanced Composite Materials

ISSN: 0924-3046 (Print) 1568-5519 (Online) Journal homepage: http://www.tandfonline.com/loi/tacm20

Out-of-plane tensile modulus of CFRP laminates by 3-point bending test

Eiichi Hara, Tomohiro Yokozeki, Hiroshi Hatta, Yutaka Iwahori & Takashi Ishikawa

To cite this article: Eiichi Hara, Tomohiro Yokozeki, Hiroshi Hatta, Yutaka Iwahori & Takashi Ishikawa (2015) Out-of-plane tensile modulus of CFRP laminates by 3-point bending test, Advanced Composite Materials, 24:3, 221-237, DOI: 10.1080/09243046.2014.960145

To link to this article: http://dx.doi.org/10.1080/09243046.2014.960145

Published online: 30 Oct 2014.

Advanced Composite Materials, 2015
Vol. 24, No. 3, 221–237, http://dx.doi.org/10.1080/09243046.2014.960145

Out-of-plane tensile modulus of CFRP laminates by 3-point bending test

Eiichi Hara[a]*, Tomohiro Yokozeki[b], Hiroshi Hatta[c], Yutaka Iwahori[a] and Takashi Ishikawa[d]

[a]*IAT, JAXA, 6-13-1 Osawa, Mitaka, Tokyo, Japan 181-0015;* [b]*Department of Aeronautics and Astronautics, University of Tokyo, 7-3-1 Hongo, Bunkyo, Tokyo, Japan 113-8656;* [c]*Space Structure and Materials Department, ISAS, JAXA, 3-1-1 Yoshinodai, Sagamihara, Kanagawa, Japan 229-8510;* [d]*Department of Aerospace Engineering, Nagoya University, Furo-cho, Chikusa-ku, Nagoya-shi, Aichi, Japan 464-8603*

(*Received 4 July 2013; accepted 26 December 2013*)

To propose a test method for the out-of-plane tensile modulus of laminated carbon fiber-reinforced plastics, 3-point bending tests using a laminated CFRP with the span direction coinciding with out-of-plane (through-the-thickness) direction were performed. It was demonstrated that the apparent bending modulus depends on the length of span to thickness ratio (L/t) and the tensile modulus E to shear modulus G ratio (E/G). Sensitivity analyses were performed to select the length of span to thickness ratio in order to evaluate the bending modulus near material modulus. Consequently, it is predicted that the bending modulus performed with the $L/t > 25$ bending specimen is equivalent to tensile modulus, if the apparent bending modulus were evaluated from 1 to 15 GPa, while modified equations for the out-of-plane modulus of QI-CFRP laminates obtained by three-dimensional laminate theory were also derived. This modification took stress condition in consideration of the small in-plane size like bending specimens into account. Moreover, it is demonstrated that apparent bending moduli were evaluated between upper and lower bound solutions. The upper bound solution is an out-of-plane modulus based on existing three-dimensional laminate theory, and the other is modified out-of-plane modulus.

Keywords: word; out of plane; mechanical properties; test method; bending test

Symbol

E	Tensile modulus
E_b	Bending modulus
G	Shear modulus
v	Poisson's ratio
E_L	Young's modulus of lamina parallel to fiber
E_T	Young's modulus of lamina in-plane transverse to fiber
E_Z	Young's modulus of lamina out-of-plane transverse to fiber
G_{LT}	Shear modulus of lamina in the LT plane
G_{LZ}	Shear modulus of lamina in the LZ plane
G_{TZ}	Shear modulus of lamina in the TZ plane

*Corresponding author. Email: Eichi12@chofu.jaxa.jp

v_{LT}	Poisson's ratio relating contraction in the T direction as a result of extension in the L direction
v_{LZ}	Poisson's ratio relating contraction in the Z direction as a result of extension in the L direction
v_{TZ}	Poisson's ratio relating contraction in the Z direction as a result of extension in the T direction
$E_{Z\text{-}QI\text{-}UD}$	Out-of-plane modulus of laminated composites having a quasi-isotropic stacking sequence, derived by the three-dimensional laminate theory
$E_{Z\text{-}QI\text{-}UD\text{-}MODIFIED}$	Out-of-plane modulus of laminated composites having a quasi-isotropic stacking sequence, derived by the modified three-dimensional laminate theory
$G_{XZ\text{-}QI\text{-}UD}$	XZ plane transverse shear modulus of laminated composites having a quasi-isotropic stacking sequence, derived by the three-dimensional laminate theory
$G_{YZ\text{-}QI\text{-}UD}$	YZ plane transverse shear modulus of laminated composites having a quasi-isotropic stacking sequence, derived by the three-dimensional laminate theory
$E_{Z\text{-}CP\text{-}UD}$	Out-of-plane modulus of laminated composites having a cross-ply stacking sequence, derived by the three-dimensional laminate theory
$E_{Z\text{-}CP\text{-}UD\text{-}MODIFIED}$	Out-of-plane modulus of laminated composites having a cross-ply stacking sequence, derived by the modified three-dimensional laminate theory
$G_{XZ\text{-}CP\text{-}UD}$	XZ plane transverse shear modulus of laminated composites having a cross-ply stacking sequence, derived by the three-dimensional laminate theory
$G_{YZ\text{-}CP\text{-}UD}$	YZ plane transverse shear modulus of laminated composites having a cross-ply stacking sequence, derived by the three-dimensional laminate theory
P	Bending load at a given point
L	Length of the support span
w	Width of the bending test specimen
t	Thickness of the bending test specimen
t_{ply}	Thickness of 1-ply lamina
Δ_s	Shear deflection in a centrally loaded bending test specimen
Δ_b	Bending deflection in a centrally loaded bending test specimen
D	Total beam deflection of the centerline of the 3-point bending specimen
σ_b	Bending stress
ε_b	Bending strain

1. Introduction

Increasing the application of composite materials, toughness CFRPs were developed with applied thermoplastic particles to interlayer, three-dimensional composites, etc. In the latest commercial aircraft, composites are used in major structural parts. It is important to evaluate both the in-plane properties and out-of-plane properties. In response to these concerns, ASTM standardized a direct out-of-plane tensile test method (ASTM D 7291[1]) for evaluating CFRP laminates. The regulation for calculating the out-of-plane

modulus involves the use of strains measured by strain gages on the side of the cylindrical specimen: either two gages separated by 180° or three strain gages 120° apart. However, this method is inadequate for evaluating the out-of-plane tensile modulus. In case of anisotropic materials, the out-of-plane strain varies with specimen thickness, diameter, and measuring position. Consequently, the out-of-plane modulus evaluated on the basis of the out-of-plane strain would also vary with these parameters [2]. Therefore, researchers reported problems, solutions, as well as an alternative solution to this test method, concerning not only the modulus but also the strength. According to these authors [2–4], the out-of-plane modulus of quasi-isotropic CFRP (QI-CFRP) laminates exceeded the modulus of aligned (unidirectional: UD) CFRP laminates and they recommended selecting a strain gage length considering the ply number and thickness [2].

The in-plane tensile modulus can be evaluated from the in-plane bending test by comparing the moduli obtained from tensile and bending tests [5]. Presumably, similar methods could also be applied to evaluate the out-of-plane tensile property. Accordingly, in this study, we proposed and demonstrated a 3-point bending test by varying the L/t ratio of UD-CFRP and QI-CFRP, which would be suitable to evaluate the out-of-plane tensile modulus accurately.

2. Relationship between bending and tensile moduli

The apparent bending modulus by the 3-point bending test varies according to the L/t ratio. This variation is caused by the fact that the total beam deflection of the centerline is the sum of the shear and bending deflection in a centrally loaded bending test specimen [6]. According to Zweben et al., the apparent bending modulus E_b by the 3-point bending test could be described by the following Equation (1) [5].

$$E_b = \frac{PL^3}{4wt^3\Delta_b(1 + \Delta_s/\Delta_b)}, \tag{1}$$

where Δ_s and Δ_b are the shear and bending deflections in a centrally loaded bending test specimen, respectively. The apparent bending modulus is similar to the tensile modulus, provided that Δ_s/Δ_b is sufficiently small. This is because, the reduction in Δ_s/Δ_b causes a reduction in the effect imposed on the bending modulus by the shear component. The Δ_s/Δ_b value can be calculated from Equation (2) [5].

$$\frac{\Delta_S}{\Delta_b} = 1.2\left(\frac{E}{G}\right)\left(\frac{1}{L/t}\right)^2. \tag{2}$$

According to this equation, the measured bending modulus is an apparent modulus dependent on E/G and L/t. In this study, the bending specimen is not a homogeneous material, since the thickness direction of the mother plate coincides with the span direction of bending specimens. However, the specimen could still be regarded as being homogeneous based on the thickness of 1 ply and a bending specimen.

3. Experiments

3.1. Material

UD-CFRP and QI-CFRP were fabricated from a unidirectionally reinforced prepreg made of reinforcing fiber IM600 and epoxy matrix #133. The thickness of 1-ply lamina was 0.145 mm. CFRP plates were fabricated by laminating 200 plies of prepreg sheets,

followed by curing at 180 °C. The resulting UD-CFRP plates were approximately 29 mm in thickness, while the stacking sequences were $[0]_{200}$ and $[(45/0/-45/90)_{25}]$ sym., and the volume fraction was 55%.

3.2. Specimen

All specimens were machined from the above-mentioned two mother plates. As shown in Figure 1, the bending specimens were machined by ensuring that the thickness direction of the mother plate coincided with that of the span. Table 1 summarizes the corresponding parameters of specimens.

3.3. Experimental procedure

The 3-point bending tests based on ASTM D 790 [7] were performed at room temperature (23 °C ± 3 °C). The radius of the loading nose was 5 mm, while that of the support nose was 2 mm. From this, the total beam deflection D of the centerline was measured. The bending strain ε_b and bending stress σ_b were calculated from Equations (3) and (4), respectively.

$$\varepsilon_b = \frac{6Dt}{L^2} \tag{3}$$

$$\sigma_b = \frac{3PL}{2wt^2} \tag{4}$$

4. Sensitivity analysis for selecting appropriate *L/t* condition

The relationship between E_b/E and L/t was discussed under the condition of the 3-point bending test for a homogeneous bending specimen. Here, E_b/E signifies the ratio of the normalized apparent bending modulus E_b to the tensile modulus E. Figure 2 shows the modulus ratio as a function of L/t and E under the condition of a constant shear modulus, G, of 2.5 GPa. Similarly, Figure 3 shows the modulus ratio as a function of

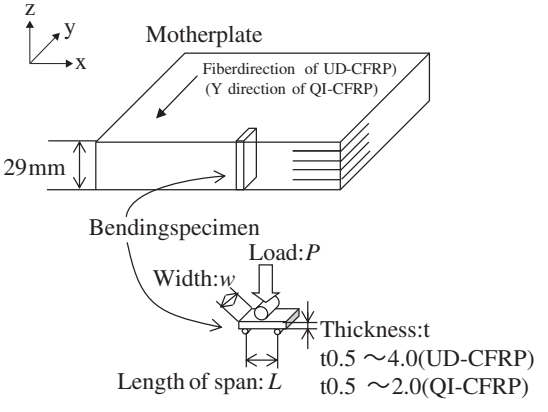

Figure 1. Specimen and CFRP mother plate.

Table 1. Parameters of specimens, number of specimens.

Stacking sequence	Length of span L mm	Thickness t mm	Length of span to thickness ratio L/t –	Number of specimen
UD	25	0.5	50	30
	25	1	25	26
	25	2	12.5	5
	25	3	8.33	5
	25	4	6.25	6
	15	0.5	30	5
	15	1	15	8
	15	3	5	4
	15	4	3.75	3
	7.5	0.5	15	6
	7.5	1	7.5	5
	7.5	2	3.75	3
	7.5	3	2.5	3
	7.5	4	1.875	2
QI	25	0.5	50	33
	25	1	25	6
	25	2	12.5	6
	15	0.5	30	5
	15	1	15	5
	15	2	7.5	5
	7.5	0.5	15	5
	7.5	1	7.5	5
	7.5	2	3.75	5

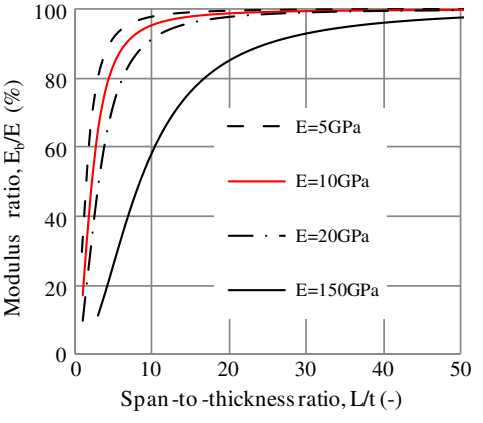

Figure 2. The modulus ratio as a function of span-to-thickness ratio (L/t).

L/t and the shear modulus G under the condition of a constant tensile modulus, E, of 15 GPa, which was defined as a high out-of-plane modulus of CFRP.

As shown in Figure 2, E_b/E exceeds 98% under conditions of $L/t > 25$ and a tensile modulus E of 5–20 GPa. As shown in Figure 3, the apparent bending modulus E_b is

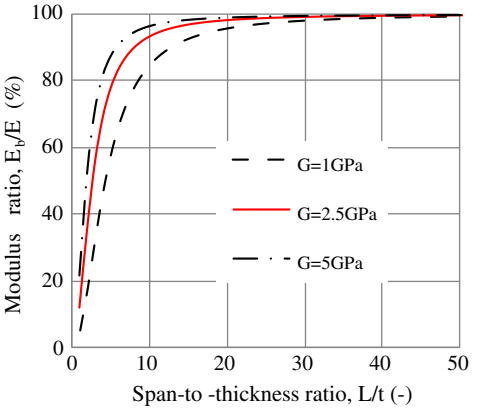

Figure 3. The modulus ratio as a function of span-to-thickness ratio (L/t).

similar to the tensile modulus E under relatively low L/t, provided that the shear modulus G increases. On the other hand, E_b/E exceeds 97% under $L/t > 25$, even though the predicted curve of the shear modulus G: 1 GPa is assumed as low shear modulus. The shear modulus G of a neat resin exceeds 1 GPa, as shown in Appendix 1. Moreover, the shear modulus G of FRP exceeds 1 GPa because the shear modulus of FRP exceeded that of a neat resin's. Therefore, it is predicted that an apparent bending modulus under 15 GPa could be regarded as the tensile modulus if measured using a bending specimen having an L/t > 25. Appendix 1 shows experimental results of the tensile test of the resin.

5. Experimental results

Figure 4 shows the typical setup for the bending test, while Figure 5 shows the stress–strain curves of UD-CFRP obtained by a bending test. The apparent bending moduli were calculated from the slope of the stress–strain curve, with a fracture stress between 25% and 50%.

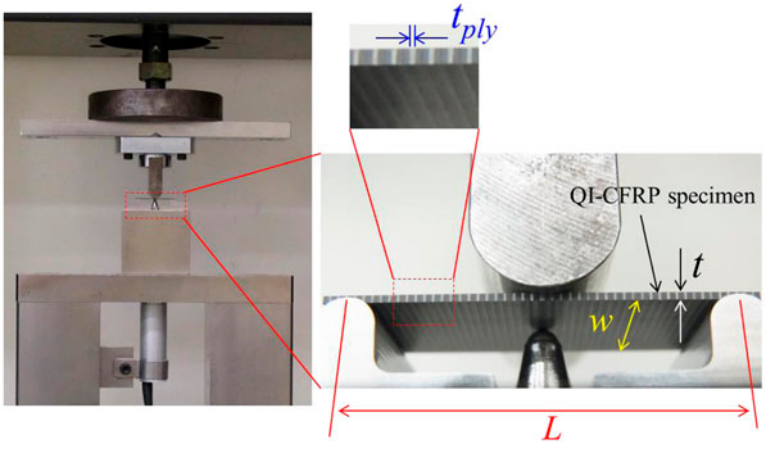

Figure 4. Test setup for bending tests.

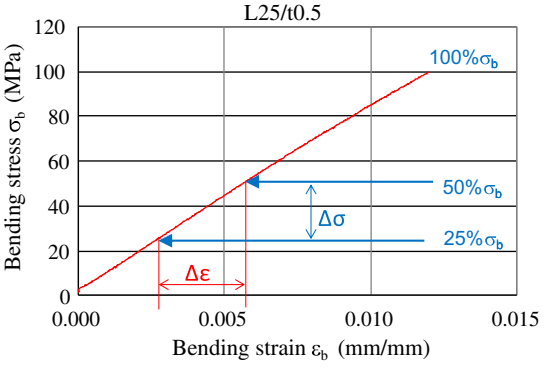

Figure 5. A typical stress–strain curve of the aligned CFRP obtained by a bending test.

Figure 6 shows the bending modulus of UD-CFRP as a function of *L*/*t*. The average of the bending modulus (8.447 GPa) under maximum L/t was decided as the out-of-plane tensile modulus, assuming that the bending modulus is similar to the tensile modulus with increasing *L*/*t*. In addition, the bending modulus vs. the *L*/*t* curve predicted by Equation (1) is also shown in Figure 6. The shear modulus *G* for prediction was used as the shear modulus G_{TZ} shown in Table 2. The corresponding predicted curves under 8.1 and 8.7 GPa are also shown in Figure 6, assuming the error of the measured modulus is 0.3 GPa. Under two conditions – *L*/*t*: 7.5/1.0 and 7.5/0.5 – the apparent bending moduli are found to be lower than the predicted curves. However, experimental results exclude the above two conditions. Table 2 shows the moduli and Poisson's ratios of UD-CFRP for calculating the out-of-plane modulus of QI-CFRP, based on the laminate theory. However, the in-plane shear modulus (G_{LT}) was taken from the Advanced Composites Database System published by the Japan Aerospace Exploration Agency [8].

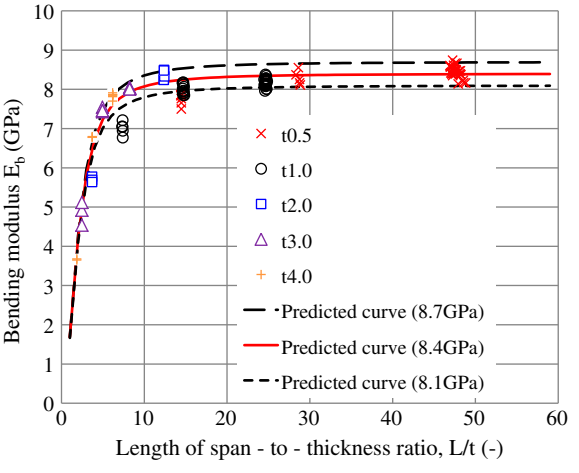

Figure 6. The bending modulus of aligned CFRP as a function of span-to-thickness ratio (*L*/*t*).

Table 2. Properties of CFRP lamina.

Property	IM600/#133	Test method	Number of specimens
E_L (GPa)	152	SACMA SRM 4R	7
E_T (GPa)	8.21	SACMA SRM 4R	6
G_{LT} (GPa)	4.36	SACMA SRM 7R	5
v_{LT}	0.334	SACMA SRM 4R	7
E_Z (GPa)	8.447	3-point bending test	30
G_{LZ} (GPa)	3.993	ASTM D 5379	10
G_{TZ} (GPa)	2.516	ASTM D 5379	10
v_{LZ}	0.346	SACMA SRM 4R	7
v_{TZ}	0.536	SACMA SRM 4R	6

Figure 7 shows the stress–strain curves of QI-CFRP obtained from the bending test, and Figure 8 shows the bending modulus of QI-CFRP as a function of L/t. In addition, two curves predicted using the out-of-plane moduli mentioned in the next section are also shown in Figure 8.

6. Discussion

6.1. *Out-of-plane modulus of QI-CFRP*

According to the three-dimensional laminate theory proposed by Gudmandson [9], Equations (5) and (6) can be directly derived for laminated composites having a QI stacking sequence: [0/45/45/90] sym. [2,9].

$$E_{Z-QI-UD} = \frac{E_Z}{1 - \frac{E_Z\{v_{TZ}E_L - v_{LZ}E_T\}^2}{E_L E_T\{E_L + (1+2v_{LT})E_T\}}} \tag{5}$$

$$G_{XZ-QI-UD} = G_{YZ-QI-UD} = \frac{2G_{LZ}G_{TZ}}{G_{LZ} + G_{TZ}} \tag{6}$$

The Cartesian coordinate system of UD-CFRP is defined as an L–T–Z coordinate system, where L, T, and Z indicate the fiber, in-plane transverse, and out-of-plane direc-

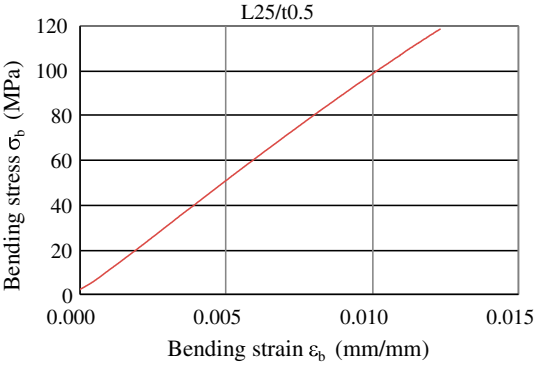

Figure 7. A typical stress–strain curves of the QI-CFRP obtained by a bending test.

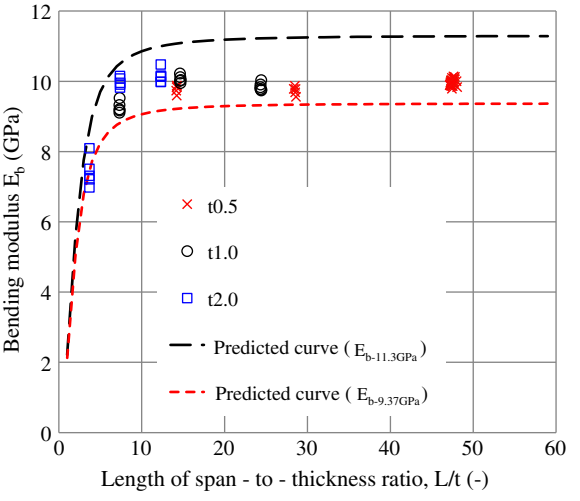

Figure 8. The bending modulus of QI-CFRP as a function of Length of span-to-thickness ratio (L/t).

tions, respectively. The X–Y–Z coordinate system is defined as the L–T–Z coordinate rotated at an optional angle around the Z-axis. By substituting the material properties from Table 2 in Equations (5) and (6), the $E_{Z\text{-}QI\text{-}UD}$ and $G_{XZ\text{-}QI\text{-}UD}$ values were determined to be 11.3 and 3.087 GPa, respectively. Appendix 2 shows a summary of the three-dimensional laminate theory by Gudmandson.

6.2. Modified QI-CFRP out-of-plane modulus

According to the experiments, the out-of-plane modulus under L/t: 50 was found to be about 10 GPa, which is lower than the theoretically calculated out-of-plane modulus (11.3 GPa). This observed difference between the experimental and theoretical values could be attributed to the following factors:

(1) The theoretical out-of-plane modulus was calculated on the basis of the assumption that the laminate is of infinite size in X–Y direction.
(2) However, under experimental conditions, the thickness of the bending specimen was small (from 0.5 to 2.0 mm), as shown in Figure 1.
(3) Therefore, the effect of increasing the out-of-plane modulus declined with decreasing stress in the in-plane X direction (thickness direction of the bending specimen).

Therefore, the modified three-dimensional laminate theory is discussed by considering a thin bending specimen. The determinant of a 6 × 6 matrix between the stress and strain of a laminate is as follows:

$$\begin{bmatrix} \sigma_X^k \\ \sigma_Y^k \\ \tau_{XY}^k \\ \sigma_Z^k \\ \tau_{XZ}^k \\ \tau_{YZ}^k \end{bmatrix} = \begin{bmatrix} Q_{11}^k & Q_{12}^k & Q_{16}^k & Q_{13}^k & Q_{15}^k & Q_{14}^k \\ & Q_{22}^k & Q_{26}^k & Q_{23}^k & Q_{25}^k & Q_{24}^k \\ & & Q_{66}^k & Q_{36}^k & Q_{56}^k & Q_{46}^k \\ & & & Q_{33}^k & Q_{35}^k & Q_{34}^k \\ & sym & & & Q_{55}^k & Q_{45}^k \\ & & & & & Q_{44}^k \end{bmatrix} \begin{bmatrix} \varepsilon_X \\ \varepsilon_Y \\ \gamma_{XY} \\ \varepsilon_Z \\ \gamma_{XZ} \\ \gamma_{YZ} \end{bmatrix} \tag{7}$$

where ε and γ, σ and τ, and k represent strain, stress, and ply number, respectively.

From this, Equation (8) could be derived by assuming the condition of plane stress for the X direction such that σ_X, τ_{XY} and $\tau_{XZ} = 0$.

$$\begin{bmatrix} 0 \\ \sigma_Y^k \\ 0 \\ \sigma_Z^k \\ 0 \\ \tau_{YZ}^k \end{bmatrix} = \begin{bmatrix} Q_{11}^k & Q_{12}^k & Q_{16}^k & Q_{13}^k & Q_{15}^k & Q_{14}^k \\ & Q_{22}^k & Q_{26}^k & Q_{23}^k & Q_{25}^k & Q_{24}^k \\ & & Q_{66}^k & Q_{36}^k & Q_{56}^k & Q_{46}^k \\ & & & Q_{33}^k & Q_{35}^k & Q_{34}^k \\ & sym & & & Q_{55}^k & Q_{45}^k \\ & & & & & Q_{44}^k \end{bmatrix} \begin{bmatrix} \varepsilon_X \\ \varepsilon_Y \\ \gamma_{XY} \\ \varepsilon_Z \\ \gamma_{XZ} \\ \gamma_{YZ} \end{bmatrix} \tag{8}$$

The determinant of a 3 × 3 stiffness matrix was derived from Equation (8).

$$\begin{Bmatrix} \sigma_Y^k \\ \sigma_Z^k \\ \tau_{YZ}^k \end{Bmatrix} = \left(\begin{bmatrix} Q_{22}^k & Q_{23}^k & Q_{24}^k \\ & Q_{33}^k & Q_{34}^k \\ sym. & & Q_{44}^k \end{bmatrix} - \begin{bmatrix} Q_{12}^k & Q_{26}^k & Q_{25}^k \\ Q_{13}^k & Q_{36}^k & Q_{35}^k \\ Q_{14}^k & Q_{46}^k & Q_{45}^k \end{bmatrix} \begin{bmatrix} Q_{11}^k & Q_{16}^k & Q_{15}^k \\ & Q_{66}^k & Q_{56}^k \\ sym. & & Q_{55}^k \end{bmatrix}^{-1} \begin{bmatrix} Q_{12}^k & Q_{13}^k & Q_{14}^k \\ Q_{26}^k & Q_{36}^k & Q_{46}^k \\ Q_{25}^k & Q_{35}^k & Q_{45}^k \end{bmatrix} \right)$$
$$\begin{Bmatrix} \varepsilon_Y^k \\ \varepsilon_Z^k \\ \gamma_{YZ}^k \end{Bmatrix} \equiv \begin{bmatrix} Q'^k_{22} & Q'^k_{23} & Q'^k_{24} \\ & Q'^k_{33} & Q'k^k_{34} \\ sym. & & Q'^k_{44} \end{bmatrix} \begin{Bmatrix} \varepsilon_Y^k \\ \varepsilon_Z^k \\ \gamma_{YZ}^k \end{Bmatrix} \tag{9}$$

Using an inverse procedure, Equation (10) was derived from Equation (9).

$$\begin{Bmatrix} \varepsilon_Y^k \\ \varepsilon_Z^k \\ \gamma_{YZ}^k \end{Bmatrix} = \begin{bmatrix} S'^k_{22} & S'^k_{23} & S'^k_{24} \\ & S'^k_{33} & S'^k_{34} \\ sym. & & S'^k_{44} \end{bmatrix} \begin{Bmatrix} \sigma_Y^k \\ \sigma_Z^k \\ \tau_{YZ}^k \end{Bmatrix} \tag{10}$$

Equation (11) in Equation (10) is defined as a modified compliance matrix.

$$\begin{bmatrix} S'^k_{II} & S'^k_{IO} \\ \left(S'^k_{IO}\right)^T & S'^k_{OO} \end{bmatrix} = \begin{bmatrix} S'^k_{22} & S'^k_{23} & S'^k_{24} \\ & S'^k_{33} & S'^k_{34} \\ sym. & & S'^k_{44} \end{bmatrix} \tag{11}$$

On the other hand, modified sub-matrices of Equation (11) were defined as follows:

$$\left[S'^k_{II}\right] = \left[S'^k_{22}\right], \tag{12}$$

$$\left[S_{IO}'^{k}\right] = \left[S_{23}'^{k} \quad S_{24}'^{k}\right], \tag{13}$$

$$\left[S_{OO}'^{k}\right] = \begin{bmatrix} S_{33}'^{k} & S_{34}'^{k} \\ S_{34}'^{k} & S_{44}'^{k} \end{bmatrix} \tag{14}$$

The modified compliance matrix of each ply was calculated, while the modified compliance matrices of the whole laminate were calculated from Equations (15), (16), and (17).

$$\bar{S}_{II}' = \left[\sum_{k=1}^{N} v^{k}\left(S_{II}'^{k}\right)^{-1}\right]^{-1} \tag{15}$$

$$\bar{S}_{IO}' = \bar{S}_{II}'\left[\sum_{k=1}^{N} v^{k}\left(S_{II}'^{k}\right)^{-1} S_{IO}'\right] \tag{16}$$

$$\bar{S}_{OO}' = \left(\bar{S}_{IO}'\right)^{T}\left(\bar{S}_{II}'\right)^{-1}\bar{S}_{IO}' + \sum_{k=1}^{N} v^{k}\left[S_{OO}'^{k} - \left(S_{IO}'^{k}\right)^{T}\left(S_{II}'^{k}\right)^{-1} S_{IO}'^{k}\right] \tag{17}$$

Equation (18) of the modified out-of-plan modulus was derived for laminated composites having an 8-ply QI stacking sequence: [0/45/45/90] sym.

$$E_{Z-QI-UD-MODIFIED} = \frac{E_Z}{1 - \frac{E_Z\{v_{TZ}E_L - v_{LZ}E_T\}^2\{E_L(3G_{LT}+E_T)+E_TG_{LT}(3-2v_{LT})\}}{E_LE_T\times 4\left\{E_L^2E_T+E_LE_T^2+E_L^2G_{LT}+E_LE_TG_{LT}(10-2v_{LT})+E_T^2G_{LT}(1-2v_{LT})\right\}}} \tag{18}$$

The modified out-of-plane modulus $E_{Z\text{-}QI\text{-}UD\text{-}MODIFIED}$ was 9.373 GPa calculated with data in Table 2.

The denominator of Equation (18) is lower than 1, similar to Equation (5).Therefore, $E_{Z\text{-}QI\text{-}UD\text{-}MODIFIED}$ exceeded E_Z. Moreover, $E_{Z\text{-}QI\text{-}UD}$ exceeded $E_{Z\text{-}QI\text{-}UD\text{-}MODIFIED}$ under the following two conditions:

$$0 < v_{LT} < 1, \tag{19}$$

$$E_T < E_L. \tag{20}$$

The inequality $E_{Z\text{-}QI\text{-}UD} > E_{Z\text{-}QI\text{-}UD\text{-}MODIFIED}$ is reasonable based on the definition.

6.3. *Relationship between experimental results and predicted curves*

Applying the $E_{Z\text{-}QI\text{-}UD}$ and $E_{Z\text{-}QI\text{-}UD\text{-}MODIFIED}$ values in Equation (1), the two predicted curves are shown in Figure 8. The experimental results include the band between the two predicted curves. With the following assumptions, the relationship between the experimental results and predicted curves is consistent:

(1) Infinite size for in-plane XY direction ($E_{Z\text{-}QI\text{-}UD}$),
(2) Thin bending specimen for in-plane X direction ($E_{Z\text{-}QI\text{-}UD\text{-}MODIFIED}$).

Even though the bending specimens had the same L/t ratio, the modulus of the thick bending specimen exceeded that of the thin bending specimen's. It is thought that the restrained condition varies with t/t_{ply}, which qualitatively affects the measured bending modulus. t/t_{ply} is lower under the condition $L7.5/t1$ than under the condition $L15/t2$ because all bending specimens in this study have the same thickness of 1-ply lamina. Thus, the bending modulus under $L7.5/t1$ was lower than that under $L15/t2$.

The ratio of the thickness of the bending test specimen to the thickness of 1-ply lamina (t/t_{ply}) is a criterion of the restrained condition for laminates. It is thought that the measured bending moduli were lower than the 11.3 GPa predicted curve in Figure 8 because of the decreasing restrained condition. Thus, the ratio of the measured bending moduli E_b to the corresponding moduli on the predicted curve $E_{b\text{-}11.3GPa}$ was calculated. Figure 9 shows the bending modulus value $E_b/E_{b\text{-}11.3GPa}$ of QI-CFRP as a function of t/t_{ply}. As evidenced from Figure 9, the $E_b/E_{b\text{-}11.3GPa}$ value decreases with decreasing t/t_{ply}. The error of $E_b/E_{b\text{-}11.3GPa}$ under the condition $L7.5/t2$ is larger than other conditions. The reason of this large error under $L7.5/t2$ is that the bending modulus significantly varies under low L/t conditions, as shown in Figure 8. These results suggest that t/t_{ply} is a criterion of the restrained condition for laminates, although limited under conditions of this study.

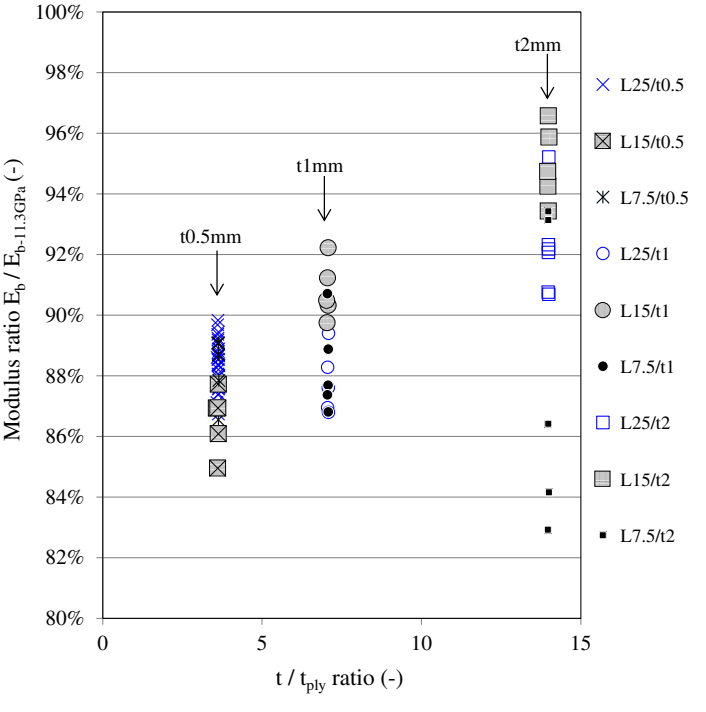

Figure 9. The bending modulus ratio of QI-CFRP as a function of specimen thickness-to-ply thickness ratio (t/t_{ply}).

$E_{Z\text{-}QI\text{-}UD}$ and $E_{Z\text{-}QI\text{-}UD\text{-}MODIFIED}$ denote the upper bound solution of the out-of-plane modulus for laminates and the lower bound solution of the out-of-plane modulus by bending test, respectively. We believe that the out-of-plane modulus using the 3-point bending test would depend on in-plane size and vary between Equations (5) and (18). The out-of-plane modulus in Equation (5) might be the out-of-plane modulus of structure because the in-plane size of the structure generally far exceeds the thickness.

6.4. Discussion of the out-of-plane modulus for the case of other stacking sequences

As for the laminate of other stacking sequences, the equations for the out-of-plane modulus, modified out-of-plane modulus, and shear modulus for cross-ply laminate were derived by Equations (21), (22), and (23), respectively.

$$E_{Z-CP-UD} = \frac{E_Z}{1 - \frac{E_Z\{\nu_{TZ}E_L - \nu_{LZ}E_T\}^2}{E_L E_T\{E_L + (1+2\nu_{LT})E_T\}}}. \tag{21}$$

$$E_{Z-CP-UD-MODIFIED} = \frac{E_Z}{1 - \frac{E_Z\{\nu_{TZ}E_L - \nu_{LZ}E_T\}^2}{E_L E_T \times 2\{E_L + E_T\}}}. \tag{22}$$

$$G_{XZ-CP-UD} = G_{YZ-CP-UD} = \frac{2G_{LZ}G_{TZ}}{G_{LZ} + G_{TZ}}. \tag{23}$$

Here, $E_{Z\text{-}CP\text{-}UD}$ agrees with $E_{Z\text{-}QI\text{-}UD}$. Using the data from Table 2, the $E_{Z\text{-}CP\text{-}UD\text{-}MODIFIED}$ value was calculated to be 9.716 GPa.

6.5. Out-of-plane moduli of UD-CFRP E_Z predicted from the bending modulus of QI-CFRP with two equations

Two E_Z were predicted from Equations (5) and (18) using the data E_L, E_T, G_{LT}, ν_{LT}, ν_{LZ}, ν_{TZ} and the bending modulus of QI-CFRP under the condition $L25/t0.5$. Accordingly, the moduli predicted by Equations (5) and (18) were 7.70 and 8.95 GPa, respectively. As compared with the out-of-plane modulus E_Z shown in Table 2, the predicted modulus from Equation (18) showed an increase of about 6%, a value lower by about 10% predicted from Equation (5). The observed error could be attributed to the following two reasons. The first reason is the difference between the two predicted curves shown in Figure 5. $E_{Z\text{-}QI\text{-}UD}$ and $E_{Z\text{-}QI\text{-}UD\text{-}MODIFIED}$ predicted the upper and lower values, respectively. The second reason is that the experimental results were included with two predicted curves. The magnitude of the error depends on several conditions, such as moduli and Poisson's ratio shown in Table 2, the size of the bending specimen and the thickness of 1-ply lamina. Although this prediction method includes the above-mentioned errors, this method predicts a value lower than E_Z with Equation (5) and a value higher than E_Z with Equation (18).

7. Concluding remark

In summary, we proposed a 3-point bending test as a standard method for measuring the out-of-plane tensile modulus of CFRP laminates. The following are some of the important conclusions derived from this study.

(1) The 3-point bending test can be used for evaluating the out-of-plane modulus.
(2) The ratio of bending and shear deformation affected the out-of-plane tensile modulus. The bending modulus became similar to the tensile modulus with increasing L/t.
(3) It was predicted and demonstrated that the apparent bending modulus could be the tensile modulus if the apparent bending modulus measured with the $L/t > 25$ bending specimen was under 15 GPa.
(4) However, the apparent moduli of QI-CFRP were included between two predicted curves: out-of-plane modulus, calculated with the existing three-dimensional laminate theory assuming infinite in-plane size, and calculated with the modified three-dimensional laminate theory assuming a thin bending specimen.
(5) The t/t_{ply} value was suggested as the criterion that affects the bending modulus between the two conditions: three-dimensional theoretical condition and modified three-dimensional theoretical condition.

References

[1] ASTM D 7291. Standard test method for through-thickness "flatwise" tensile strength and elastic modulus of a fiber-reinforced polymer matrix composite material. American Society for Testing and Materials; 2007.
[2] Hara E, Yokozeki T, Hatta H, Iwahori Y, Ishikawa T. CFRP laminate out-of-plane tensile modulus determined by direct loading. Composites Part A. 2010;41:1538–1544.
[3] Hara E, Yokozeki T, Hatta H, Ishikawa T, Iwahori Y. Effects of geometry and specimen size on out-of-plane strength of aligned CFRP determined by direct tensile method. Composites Part A. 2010;41:1425–1433.
[4] Hara E, Yokozeki T, Hatta H, Iwahori Y, Ogasawara T, Ishikawa T. Comparison of out-of-plane tensile strengths of aligned CFRP obtained using the 3-point bending and direct loading tests. Composites Part A. 2012;43:1828–1836.
[5] Zweben C, Smith WS, Wardle MW. Test methods for fiber tensile strength, composite flexural modulus, and properties of fabric-reinforced laminates. ASTM STP 674 Composite Materials: Testing And Design (Fifth Conference); 1979. pp. 228–262.
[6] Timoshenko S, Young DH. Elements of strength of materials. 5th ed. D. Van Nostrand: Princeton, NJ; 1968 (translated Japanese version by Maezawa S, Corona publishing, 1972. pp. 227–232).
[7] ASTM D 790. Standard test methods for flexural properties of unreinforced plastics and electrical insulating materials. American Society for Testing and Materials; 2007.
[8] Advanced composites database system. JAXA-ACDB, Ver.06-1. http://www.jaxa-acdb.com/.
[9] Gudmundson P, Zang W. J. Solid Struct. 1993;30:3211–3231.
[10] JIS K 7161-1994 Plastics – Determination of tensile properties – Part 1: General principles Japanese Standards Association; 1994.

Appendix 1. Resin properties by tensile tests

Tensile tests for the matrix resin were carried out on the basis of JIS K 7161[10]. In a typical procedure, a dumbbell-type specimen and a coupon-type specimen were prepared as shown in Figure A1. The test speed was 1.0 mm/min. Two biaxial strain gages (gage length 3 mm) were

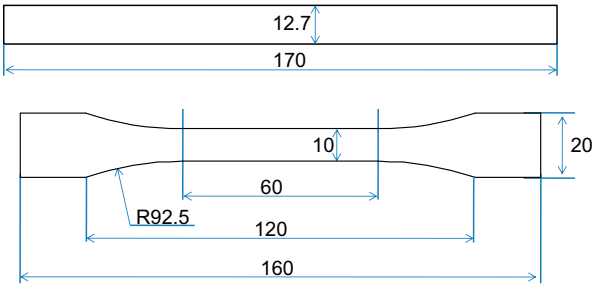

Figure A1. Geometry of tensile test specimens for matrix resin.

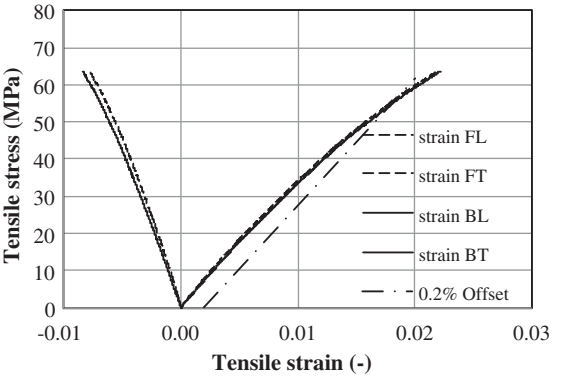

Figure A2. Typical stress–strain curves of neat resin #133 obtained by the dumbbell type tensile test.

Table A1. Properties of epoxy resin 133.

Property	Unit	Test method	Number of Specimens	Coupon	Dumbbell	Error between coupon and dumbbell
Strength	MPa	JIS K 7161	5	69.6	67.0	3.9%
0.2% offset strength	MPa		5	54.1	53.3	1.5%
Tensile modulus	GPa	JIS K 7161	5	3.520	3.622	2.8%
Poisson's ratio	–	JIS K 7161	5	0.376	0.365	3.0%
Shear modulus	GPa	An assumption $G = E/\{2(1+\nu)\}$		1.279	1.327	3.6%

glued on the surfaces of both sides of the specimen. Figure A2 shows the stress–strain curves of neat resin #133 obtained by the dumbbell-type tensile test. The tensile moduli were calculated with a stress–strain slope between 0.0025 and 0.0050 of the tensile strain, while the offset strength of 0.2% was also calculated on the basis of the elastoplasticity of resin. Table A1 shows the experimental results of the resin material. The error rate for experimental results between the dumbbell and coupon was 4% or less. Calculated shear moduli are shown in Table A1, assuming isotropy of the resin material.

Appendix 2. Derivation of the out-of-plane modulus by the three-dimensional laminate theory

The Cartesian coordinate system of UD-CFRP is defined as an *L–T–Z* coordinate system, where *L*, *T,* and *Z* indicate the fiber, in-plane transverse, and out-of-plane directions, respectively. The *X–Y–Z* coordinate system is defined as the *L–T–Z* coordinate rotated at an optional angle θ around the *Z*-axis. The global average stresses and strains are defined as follows

$$[\bar{\varepsilon}] \equiv \begin{bmatrix} \bar{\varepsilon}_I \\ \bar{\varepsilon}_O \end{bmatrix}, \tag{A1a}$$

$$[\bar{\sigma}] \equiv \begin{bmatrix} \bar{\sigma}_I \\ \bar{\sigma}_O \end{bmatrix}, \tag{A1b}$$

where *I* is the in-plane component, *O* is the out-of-plane component, and

$$.[\bar{\varepsilon}_I] = \begin{bmatrix} \bar{\varepsilon}_X \\ \bar{\varepsilon}_Y \\ \bar{\varepsilon}_{XY} \end{bmatrix}, \tag{A2a}$$

$$[\bar{\sigma}_I] = \begin{bmatrix} \bar{\sigma}_X \\ \bar{\sigma}_Y \\ \bar{\sigma}_{XY} \end{bmatrix}. \tag{A2b}$$

are in-plane stress, and strains and

$$[\bar{\varepsilon}_O] = \begin{bmatrix} \bar{\varepsilon}_Z \\ \bar{\varepsilon}_{XZ} \\ \bar{\varepsilon}_{YZ} \end{bmatrix}, \tag{A3a}$$

$$[\bar{\sigma}_O] = \begin{bmatrix} \bar{\sigma}_Z \\ \bar{\sigma}_{XZ} \\ \bar{\sigma}_{YZ} \end{bmatrix}. \tag{A3b}$$

are out-of-plane strains and stresses.

The relationship between global effective stresses and strains is as follows:

$$\begin{bmatrix} \bar{\varepsilon}_I \\ \bar{\varepsilon}_O \end{bmatrix} = \begin{bmatrix} \bar{S}_{II} & \bar{S}_{IO} \\ (\bar{S}_{IO})^T & \bar{S}_{OO} \end{bmatrix} \begin{bmatrix} \bar{\sigma}_I \\ \bar{\sigma}_O \end{bmatrix}. \tag{A4}$$

where $\bar{S}_{II}$ etc. are the corresponding 3 × 3 sub-matrices. For laminates with *N* ply, the global average stresses and strains are defined as follows

$$\bar{\varepsilon} = \sum_{k=1}^{N} v^k \varepsilon^k, \tag{A5a}$$

$$\bar{\sigma} = \sum_{k=1}^{N} v^k \sigma^k, \tag{A5b}$$

$$\sum_{k=1}^{N} v^k = 1. \tag{A5c}$$

where, v^k is the volume fraction of ply k. Assuming that in-plane strains and out-of-plane stresses are equal to average global strains and stresses, respectively,

$$\varepsilon_I^k = \bar{\varepsilon}_I, \tag{A6a}$$

$$\sigma_O^k = \bar{\sigma}_O. \tag{A6b}$$

As for each ply of the laminate, the stress and strain equations were derived by the following equation:

$$\begin{bmatrix} \varepsilon_I^k \\ \varepsilon_O^k \end{bmatrix} = \begin{bmatrix} S_{II}^k & S_{IO}^k \\ \left(S_{IO}^k\right)^T & S_{OO}^k \end{bmatrix} \begin{bmatrix} \sigma_I^k \\ \sigma_O^k \end{bmatrix}. \tag{A7}$$

Equation (A8) was given by Equations (A7) and (A6).

$$\sigma_I^k = \left(S_{II}^k\right)^{-1}\left(\bar{\varepsilon}_I - S_{IO}^k \bar{\sigma}_O\right) \tag{A8}$$

Equation (A9) was calculated by substituting Equation (A8) in Equations (A5a–A5c),

$$\bar{\sigma}_I = \left(\sum_{k=1}^{N} v^k \left(S_{II}^k\right)^{-1}\right)\bar{\varepsilon}_I - \left(\sum_{k=1}^{N} v^k \left(S_{II}^k\right)^{-1} S_{IO}^k\right)\bar{\sigma}_O. \tag{A9}$$

Equations (A10) and (A11) were derived by comparing the Equations (A7) and (A9),

$$\bar{S}_{II} = \left[\sum_{k=1}^{N} v^k \left(S_{II}^k\right)^{-1}\right]^{-1} \tag{A10}$$

$$\bar{S}_{IO} = \bar{S}_{II}\left[\sum_{k=1}^{N} v^k \left(S_{II}^k\right)^{-1} S_{IO}^k\right] \tag{A11}$$

An out-of-plane sub-matrix was also derived from Equations (A7) and (A5a–A5c),

$$\bar{S}_{OO} = \left(\bar{S}_{IO}\right)^T \left(\bar{S}_{II}\right)^{-1} \bar{S}_{IO} + \sum_{k=1}^{N} v^k \left[S_{OO}^k - \left(S_{IO}^k\right)^T \left(S_{II}^k\right)^{-1} S_{IO}^k\right] \tag{A12}$$

The inverse of the components of the first row and first column of the matrix is an out-of-plane modulus. For example, Equation (5) can be directly derived for laminated composites having a QI stacking sequence: [45/0/-45/90] sym.